



Published in final edited form as:

J Biomech. 2008 ; 41(5): 1095–1103.

Compressive forces induce osteogenic gene expression in calvarial osteoblasts

Bjoern Rath¹, Jin Nam¹, Thomas J Knobloch¹, John J Lannutti², and Sudha Agarwal^{1,*}

¹ Biomechanics and Tissue Engineering Laboratory, The Ohio State University, Columbus, OH 43210

² Department of Materials Science and Engineering, The Ohio State University, Columbus, OH 43210

Abstract

Bone cells and their precursors are sensitive to changes in their biomechanical environment. The importance of mechanical stimuli has been observed in bone homeostasis and osteogenesis, but the mechanisms responsible for osteogenic induction in response to mechanical signals are poorly understood. We hypothesized that compressive forces could exert an osteogenic effect on osteoblasts and act in a dose-dependent manner. To test our hypothesis, electrospun poly(ϵ -caprolactone) (PCL) scaffolds were used as a 3-D microenvironment for osteoblast culture. The scaffolds provided a substrate allowing cell exposure to levels of externally-applied compressive force. Pre-osteoblasts adhered, proliferated and differentiated in the scaffolds and showed extensive matrix synthesis by Scanning Electron Microscopy (SEM) and increased Young's modulus (136.45 ± 9.15 kPa) compared to acellular scaffolds (24.55 ± 8.5 kPa). Exposure of cells to 10% compressive strain (11.81 ± 0.42 kPa) resulted in a rapid induction of bone morphogenic protein-2 (*BMP-2*), runt-related transcription factor 2 (*Runx2*), and MAD homolog 5 (*Smad5*). These effects further enhanced the expression of genes and proteins required for extracellular matrix (ECM) production, such as alkaline phosphatase (*Akp2*), collagen type I (*Col1a1*), osteocalcin/bone gamma carboxyglutamate protein (*OC/Bglap*), osteonectin/secreted acidic cysteine rich glycoprotein (*ON/Sparc*) and osteopontin/secreted phosphoprotein 1 (*OPN/Spp1*). Exposure of cell-scaffold constructs to 20% compressive strain (30.96 ± 2.82 kPa) demonstrated that these signals are not osteogenic. These findings provide the molecular basis for the experimental and clinical observations that appropriate physical activities or microscale compressive loading can enhance fracture healing due in part to the anabolic osteogenic effects.

Keywords

Osteoblast; Scaffold; Compression; Gene Expression; Osteogenic

1. Introduction

Biomechanical signals are essential for bone homeostasis, growth, adaptation, healing and remodeling; a lack of such signals leads to bone loss (Bikle and Halloran, 1999; Ehrlich and Lanyon, 2002). Mechanical stimuli in bone are transmitted through the ECM to resident osteoblasts, osteocytes, periosteal cells and osteoclasts (Cowin, 1999; Klein-Nulend et al.,

*Corresponding author: Sudha Agarwal, Ph.D. Biomechanics and Tissue Engineering Laboratory 4010 Postle Hall The Ohio State University, Columbus OH 43210 Tel: 614-537-6986 Fax: 614-247-7475 E-mail: agarwal.61@osu.edu.

Publisher's Disclaimer: This is a PDF file of an unedited manuscript that has been accepted for publication. As a service to our customers we are providing this early version of the manuscript. The manuscript will undergo copyediting, typesetting, and review of the resulting proof before it is published in its final citable form. Please note that during the production process errors may be discovered which could affect the content, and all legal disclaimers that apply to the journal pertain.

2005; Rubin et al., 2006). Responses of osteoblasts to mechanical signals are attributed to the deformation of the cells and its surrounding matrix (Damsky, 1999; Klein-Nulend et al., 2005). Both animal and clinical studies have consistently shown the anabolic effects of compressive forces on bone as well as increased mineralization and fracture stiffness during fracture healing (Klein-Nulend et al., 1987; MacKelvie et al., 2003; Rubin et al., 2001; Chao et al., 1998; Egger et al., 1993; Gardner et al., 2006; Goodship et al., 1998; Kenwright and Goodship, 1989). The mechanisms by which these signals control osteogenesis remain elusive. In this study, we used a 3-D PCL scaffold to investigate the effect of compressive forces on osteogenic markers in 4 weeks cultured pre-osteoblasts. Studies have shown that 3-D scaffolds can support osteoblast differentiation and mineralization (Cao et al., 2003; Ishaug et al., 1997). Furthermore, long term compressive forces induced mineralization while oscillation accelerated differentiation of osteoblastic cells (Gabbay et al., 2006; Visconti et al., 2004). Such studies are highly instructive and point out the need to investigate well-defined applied compressive forces that allow deliberate, systematic application of mechanical stresses to aid in tissue remodeling.

Bone morphogenetic protein-2 (BMP-2) plays a major role in this process and stimulates both osteoblast proliferation and differentiation (ten Dijke, 2006). The up-regulation of BMP-2 results in the acetylation of RUNX2, leading to increases in the transactivational activity and inhibition of degradation of RUNX2 (Jeon et al., 2006). The expression of RUNX2 represents a molecular biomarker signaling pre-osteoblastic cell differentiation along the osteoblastic lineage and continues to modulate bone formation by regulating the activity of differentiated osteoblasts (Ducy, 2000). BMP-2 binding to its receptors activates the transcription factors SMAD1 and/or SMAD5 (Ryoo et al., 2006). Both RUNX2 and SMADs are essential for the synthesis of proteins important during osteogenesis. RUNX2 induces the expression and synthesis of *OC/Bglap*, *OPN/Spp1* and *Colla1*, while activation of RUNX2 and SMAD5 induces *Akp2* expression (Ducy et al., 1997; Harada et al., 1999; Lee et al., 2000).

In this report, we have investigated well-defined mechanotransduction as a means of promoting osteogenesis by examining the resulting expression of proteins and transcription factors known to be essential for osteogenic differentiation and functional maturation. We show that compressive forces were effective up-regulators of osteogenesis by inducing *Bmp-2*, *Runx2* and *Smad5* expression, and resulted in the enhanced synthesis of proteins required for matrix deposition.

2. Materials and methods

2.1. Scaffold synthesis

A 15 wt. % solution of poly(ϵ -caprolactone) (PCL, M_w 65,000, Aldrich, St. Louis, MO) in dichloromethane (Mallinckroff Chemicals, Phillipsburg, NJ) was electrospun at 20 kV using a FC50R2 DC power supply (Glassman High Voltage Inc., High Bridge, NJ) at a flow rate of 15 ml/h and a tip-to-substrate distance of 30 cm. The electrospun PCL fiber meshes, 3mm thick with a porosity of 90% were treated in a vacuum oven (<30 mm Hg) at 45°C for 24 hours to remove residual solvents (Nam et al., 2007b). The average diameter of as-spun fibers was approximately 10 μ m, and distinctive nanopores were present on the fiber surface. Cylindrical scaffolds were formed with a 6.0 mm diameter biopsy punch (Miltex Inc., York, PA), sterilized in 70% ethanol, washed three times with PBS, and soaked in tissue culture medium (TCM) for two days to improve hydrophilicity.

2.2. Cell culture

Calvariae were harvested from 3-day-old Sprague Dawley rats following protocols approved by the IACUC at The Ohio State University. Calvariae were cleaned, minced, and digested in

0.2% collagenase I (Worthington Biochemical, Corp., Lakewood, NJ) twice for 10 min and twice for 20 min at 37°C. The first digestion supernatant was discarded. Thereafter, each supernatant containing cells was collected by centrifugation at 500xg, pooled and resuspended in TCM [DMEM (Invitrogen Corp., Carlsbad, CA), 10% FBS (Atlanta Biologicals, Lawrenceville, GA), 100 units penicillin G, 100 µg/mL streptomycin sulphate, 0.25 µg/mL Amphotericin B (Invitrogen) and 2 mM L-glutamine (Invitrogen)]. Cells (2×10^6 cells/ 75cm^2) were cultured in TCM at 37°C, 5% CO₂, and 90% humidity and passages 3–6 were used.

A total of 2×10^5 cells / 40 µl of TCM were seeded into each scaffold. After 2 hours, additional 2 ml of TCM were added. The TCM was replaced every two days, and cells were grown in scaffolds for 4 weeks and phenotyped for osteoblastic markers prior to compression.

2.3. Mechanical testing

The mechanical properties of acellular and cell-seeded/cultured scaffolds were measured using a 1 kg load cell (Honeywell Sensotec, Chardon, OH) on a load frame (TestResources Inc., Shakopee, MN) at 10 or 20% compressive strain. A saw-tooth profile at a frequency of 0.5 Hz was used. Prior to measurements, acellular samples were soaked in TCM overnight. The mechanical testing was performed on specimens submerged in TCM.

2.4. Application of dynamic compression

Following 4 weeks of culture, cell-scaffold constructs were subjected to cyclical unconfined compression at 0.5 Hz with a saw-tooth profile for 4 hours using a custom-designed computer-controlled device in an incubator at 37°C. The cell-scaffold constructs were exposed to 10 or 20% dynamic compressive strain with a pre-loading of approximately 2.5 g and uncompressed samples were used as controls. These samples did not exhibit loading platen liftoff during the entire period of the dynamic compression as observed by mechanical testing. To determine the loss of cells from the scaffolds during the compression regimes, the culture supernatants were collected, centrifuged and examined for the presence of cells released from the scaffolds. Exposure of cell-scaffolds constructs to compression for 4 hours did not dislocate cells from the scaffolds as evidenced by the absence of cells in the surrounding medium or culture plates. Furthermore, the total yields of RNA and proteins from the cell-scaffold constructs with or without exposure to compression were practically equal.

2.5. Von Kossa staining

Four weeks as-cultured cell-scaffold constructs were fixed with 10% formalin (Richard-Allen Scientific, MI). The cell-scaffold constructs were then stained with von Kossa stain as described earlier (Luna, 1968) and counterstained with nuclear fast red.

2.6. Scanning electron microscopy (SEM)

The SEM sample preparation was carried out as described previously (Nam et al., 2007a). Cell-scaffold constructs cultured for 4 weeks as-cultured and after 4 hours at 10% compression were fixed with 10% formalin (Richard-Allen Scientific). The fixed samples were dehydrated using a graded series of ethanol in DI water (50, 70, 85, 90 and 100% ethanol), followed by a graded series of ethanol-hexamethyldisilazane (HMDS, Electron Microscopy Sciences, PA) solutions (25, 50, 75 and 100% HMDS). The dehydrated samples were coated with an 8 nm thick layer of osmium (OPC-80T, SPI Supplies, PA) prior to SEM observation using an FEI XL-30 Sirion SEM (FEI Company, Hillsboro, OR) with a field emission gun (FEG) at a voltage of 5 kV and with a working distance of 15 mm.

2.7. Analysis of gene expression

Total RNA was extracted from the cell-scaffold constructs using the RNeasy Kit (Qiagen Inc, Valencia, CA) immediately after compression. A total of 1 µg of RNA was reverse transcribed using the Superscript III Reverse Transcriptase Kit (Invitrogen).

Expression of *OC/Bglap* and *Akp2* was detected by end-point RT-PCR as described earlier (Deschner et al., 2006). Custom-designed (Primer Express, Applied Biosystems, Foster City, CA), gene-specific primers (Table 1) were used to amplify the cDNA in Platinum PCR SuperMix (Invitrogen).

Regulation of gene expression by compressive forces was analyzed by performing real-time RT-PCR using the Bio-Rad iCycler iQ (Hercules, Ca). The cDNA was amplified with the SYBR Green Supermix (Biorad) and gene-specific primers (Table 1) in a 25 µl reaction. The thermocycling protocol was: 95°C for 3 min, 40 cycles of denaturation at 95°C for 30 s, annealing at 60°C for 30 s, and extension at 72°C for 30 s. Ribosomal Protein S18 (*Rps18*) was used as an internal control. Melt curve analyses were performed on each primer set to minimize primer-dimers and non-specific products. The data were analyzed by the comparative threshold cycle (C_T) method (Livak and Schmittgen, 2001).

2.8. Western blot analysis

The proteins were analyzed from whole cell lysates of uncompressed and compressed cells (4 hours of 10% compression at 0.5 Hz followed by 8 hours of rest). Protein concentration was measured using BCA Protein Assay Reagent (Pierce Biotechnology, Rockford, IL) and VICTOR³ plate reader (PerkinElmer, Waltham, MA). The measurement showed equal amounts of total proteins out of control and compressed cell-scaffold constructs. Equal amounts of protein were resolved through SDS-10%-PAGE and electrotransferred onto nitrocellulose membranes (Bio-Rad Laboratories). The membranes blocked with 5% nonfat milk were probed with mouse anti-rat OPN/SPPI or rabbit anti-rat ON/SPARC antibodies (Santa Cruz Biotechnology, Santa Cruz, CA). Proteins were normalized by probing the membranes for anti-rat β-actin. Binding of primary antibodies was revealed with IRDye 800CW- or IRDye 680-conjugated secondary antibodies (LI-COR Biosciences, Lincoln, NE). The membranes were analyzed using the Odyssey Infrared Imaging System and software (LI-COR Biosciences) at 680 nm and 800 nm using a 169 µm resolution.

2.9. Statistical analysis

SPSS 15.0 software (SPSS Inc., Chicago, IL) was used for statistical analysis. To quantitatively analyze the gene expression, mean values and standard errors of the mean (S.E.M.) were calculated. Each experiment was performed at least three times (n=6/group). One-Way Analysis of Variance (ANOVA) and the *post hoc* multiple comparison Tukey's test were applied. For quantitative analysis of the protein syntheses, mean values and S.E.M. were calculated (n=3/group) and Student's T-test was performed. Results were considered statistically significant at $p < 0.05$.

3. Results

3.1. Osteoblast growth, matrix synthesis and mineralization in 3-D scaffolds

Gene expression analysis by end-point PCR of uncompressed cell-scaffold constructs showed expression of *Akp2* and *OC/Bglap*, confirming their osteoblastic phenotype (Fig. 1A (i), (ii)). Mineralized tissue was shown by von Kossa staining in the scaffolds after 4 weeks of culture (Fig. 1A (iii) and B).

SEM provided evidence of cell anchorage and matrix deposition in both untreated control cell-scaffold constructs and those exposed to 10% compression. All cell-scaffold constructs displayed matrix deposition (Fig. 1C) and examination of the internal area revealed that these scaffolds allowed marked cell growth and matrix deposition in that area as well (Figs. 1D-F). The osteoblasts appeared to be anchored to the PCL fibers via the nanopores on their surface (Fig. 1E). Higher magnification revealed interconnections between the PCL fibers and the ECM (Fig. 1F). However, there were no morphological differences between the compressed and uncompressed samples.

3.2. Mechanical testing of acellular and cellular scaffolds

We next determined whether the mechanical properties of the scaffolds were altered by cell proliferation/ECM deposition after 4 weeks of culture. Therefore, cellular scaffolds placed in TCM overnight and scaffolds in which cells were grown for 4 weeks were subjected to mechanical testings in various levels of compression (Fig. 2). Acellular scaffolds exposed to 10% compression at a frequency of 0.5 Hz exhibited a peak stress of 2.05 (± 0.63) kPa. Acellular scaffolds exposed to 20% compressive strain at 0.5 Hz exhibited a peak stress of 5.72 (± 2.14) kPa. The cell-scaffold constructs after 4 weeks of culture showed a peak stress of 11.81 (± 0.42) kPa following exposure to 10% compression at 0.5 Hz, and a peak stress of 30.96 (± 2.82) kPa following 20% compressive strain at 0.5 Hz. Calculations of mechanical strength under both conditions revealed that cell-scaffold constructs displayed an increased Young's modulus for compression of cellular scaffolds (136.45 ± 9.15 kPa) compared to that of acellular scaffolds (24.55 ± 8.5 kPa) (Fig. 2). This increase in the Young's modulus can be directly attributed to the ECM deposition by adherent cells. Furthermore, the cellular scaffolds achieved viscoelastic behavior based on the character of the hysteresis loops during the loading and unloading cycles (Fig. 2).

3.3. Compressive forces upregulate BMP-2, RUNX2, SMAD1 and SMAD5 expression

BMP-2 is one of the signals involved in osteogenesis. Interestingly, exposing cells to both 10 and 20% compressive strain up-regulated *Bmp-2* gene expression significantly ($p < 0.05$). However, there was no significant difference between cells exposed to 10 or 20% compression (Fig. 3A). Next, we determined the effect of compressive forces on the expression of *Runx2*. Fig. 3B demonstrates that exposure of cells to 10% compression led to a significant ($p < 0.05$) increase in *Runx2* mRNA expression. However, 20% compression inhibited *Runx2* mRNA expression below control levels. We next examined whether up-regulation of *Bmp-2* resulted in the up-regulation of *Smad1* or *Smad5* expression. Compression at 10% significantly ($p < 0.05$) induced *Smad5* expression above those of untreated controls and cells exposed to 20% compression. Expression of *Smad5* in cells exposed to 20% compressive forces was not significantly greater than uncompressed control cells (Fig. 3D). *Smad1* expression was increased after both 10 and 20% compression but only 20% compression significantly ($p < 0.05$) up-regulated expression over controls (Fig. 3C).

3.4. Compressive forces up-regulate the expression of alkaline phosphatase and collagen type I

We examined whether the induction of *Bmp-2* and *Runx2* by compressive forces is paralleled by the expression of *Colla1* and *Akp2* mRNA in cells subjected to compression. The expression of both markers was significantly ($p < 0.05$) up-regulated by compressive strains of 10% as compared to both uncompressed control cells and cells exposed to 20% compression (Fig. 4A and B). However, compressive strains of 20% did not increase the gene expression of *Akp2* and *Colla1* significantly over controls.

3.5. Regulation of non-collagenous bone matrix proteins by compressive forces

Compressive forces of 10% strain at 0.5 Hz significantly ($p < 0.05$) up-regulated *OC/Bglap* expression over untreated control cells, whereas 20% compression inhibited the expression of the *OC/Bglap* as compared to controls (Fig. 5A). Significant up-regulation in the expression of *OPN/Spp1* and *ON/Sparg* was also observed following exposure to 10% compression; however, 20% compression did not increase *OPN/Spp1* expression over controls. *ON/Sparg* expression after 20% compression was lower than that observed in response to 10% compression (Fig 5B and C). We next determined whether the protein synthesis of OPN/SPP1 and ON/SPARC were up-regulated in parallel to mRNA expression by Western blot analysis. As shown in Fig. 5 D and E, 10% compression at 0.5 Hz up-regulated protein syntheses of OPN/SPP1 and ON/SPARC significantly above those of untreated control cells ($p < 0.05$).

4. Discussion

In this report we have shown that pre-osteoblasts proliferated and deposited ECM in 3-D macrofibrous PCL scaffolds. After 4 weeks of culture, SEM showed extensive matrix deposition by cells grown in 3-D PCL scaffolds. The cells resided in the ECM contained within the pores of the PCL mesh. The presence of mineralized residues, as shown by von Kossa stain further confirmed that the 3-D environment was conducive to osteogenesis, similar to that observed in an earlier study (Ishaug et al., 1997). In addition, trends in mechanical properties confirmed that these 3-D cultures benefited from exhibited matrix synthesis as is evident from the increased Young's modulus and their viscoelastic characteristics. Culture of pre-osteoblasts in this 3-D environment enhanced the osteoblastic phenotype as evident by the expression of *OC/Bglap* and *Akp2*. Thus, scaffolds provided a suitable environment for pre-osteoblasts to proliferate and differentiate into osteoblasts in the absence of differentiation medium containing ascorbate acid and β -glycerolphosphate. A similar enhanced osteoblast differentiation was observed in 3-D collagen type I gels and polymer scaffolds (Ishaug et al., 1997; Kinoshita et al., 1999; Masi et al., 1992).

Dynamic compression caused the deformation of the cell-scaffold constructs. This deformation of ECM and the scaffold fibers apparently led to beneficial mechanical stimulation of the cells. In this system, while the majority of applied forces were compressive, cells also experienced fluid shear as well as tensile forces due to the open, highly compliant nature of these macroporous fiber meshes (Johnson et al., 2007) and the attendant deposition of matrix. Therefore, such long term culture of cell-scaffold constructs provided a system that recapitulates the *in vivo* environment in which native osteoblasts experience such a wide range of forces. By using this 3-D system we have shown that compressive forces are potent osteogenic signals that induced rapid induction of osteogenic genes and proteins within 4 hours. This increase in the osteogenic gene induction could not be attributed to increase in cell proliferation, as the mRNA analysis was conducted immediately after 4 hours of compression.

The effects of mechanical stimuli on osteoblastic cell types have been studied in 2-D culture by applying cyclic tensile strain (stretch) (Kaspar et al., 2000; Koike et al., 2005; Ziros et al., 2002) or compression (Klein-Nulend et al., 1997; Roelofsen et al., 1995; Visconti et al., 2004). Furthermore, studies used 3-D culture systems to observe the effects of biomechanical forces on osteoblastic cells (Cartmell et al., 2003; Duty et al., 2007; Gabbay et al., 2006; Tanaka et al., 2005). Other studies observed cell growth in 3-D cultures in the absence of any mechanical stimuli (Cao et al., 2003; Ishaug et al., 1997). Here we show that direct dynamic compression on osteoblasts cultured in a 3-D environment up-regulated bone specific differentiation markers in osteoblasts and spotlights the potentially crucial role of mechanical signals during osteoblast differentiation. Increased bone mineralized was reported after 3 days of compression at 0.05 Hz followed by 18 days rest (Visconti et al., 2004) and after 2 weeks of 20–200 psi compression at 1 Hz for 30 min / day of polymer scaffolds subcutaneously

implanted in rats (Duty et al., 2007). Due to the fact that we used only short-term mechanical loading in our study, bone mineralization immediately at the conclusion of loading was not investigated.

Up-regulation of BMP-2 by compressive forces can induce signals to regulate proliferation and differentiation of osteoblasts in an autologous manner. Furthermore, its expression at both 10 and 20% compression suggests that its expression may be up-regulated by physiologic as well as hyper-physiologic loadings. In fact, *in vivo* studies have shown that BMP-2 is up-regulated during fracture healing (Einhorn, 1998; Phillips, 2005) and rhBMP-2 has been clinically used to improve bone healing (Govender et al., 2002). Thus, our findings reinforce the regenerative capacity of compressive forces, and predict that it may be mediated via autogenous up-regulation of BMP-2 in response to these mechanical forces.

RUNX2 is a transcription factor essential for osteoblast differentiation (Lian et al., 2004). We have observed that 10 but not 20% compression up-regulates *Runx2* expression. Similarly, fluid shear forces and cyclic tensile strain also up-regulated *Runx2* in monolayer cultures (Koike et al., 2005; Ziros et al., 2002).

SMAD1 and SMAD5 translocate to the nucleus in response activation by BMP-2 (Wan and Cao, 2005). Compressive forces with 10 but not 20% strain markedly up-regulated *Smad5* expression. An identical relationship between strain and *Akp2* expression exists. In this regard, SMAD5 induced *Akp2* expression (Ryoo et al., 2006); therefore it is not surprising that compressive forces up-regulated *Akp2* in parallel to *Smad5*. *Smad1* was up-regulated by both 10 and 20% compressive strain. Collectively, these findings suggest that BMP-2 up-regulation by 20% compression is not paralleled by *Runx2* and *Smad 5* expression, and thus the effects of BMP-2 following 20% compression may be regulated by *Smad1*, suggesting its importance during repair after injury due to high mechanical loading.

Up-regulation of *Akp2*, a hydrolase enzyme important during matrix deposition, and *Coll1a1*, the major extracellular bone protein, by compressive forces reinforced the osteogenic potential of compressive forces. OC/BGLAP, the most abundant protein in bone, is a mature osteoblastic marker and its expression correlates with bone formation (Bilezikian et al., 2002; Fernández-Tresguerres-Hernández-Gil et al., 2006; Hall, 2005). Up-regulation of *OC/Bglap* expression has been reported under cyclic tensile strain after 9 days (Mikuni-Takagaki et al., 1996) and up-regulation of *Akp2* and *OC/Bglap* was shown under periodic distraction and compression of collagen type I gels after 8 days (Gabbay et al., 2006). However, *OC/Bglap* expression has not been shown to be up-regulated by mechanical strain in other studies (Kaspar et al., 2000; Koike et al., 2005). In contrast, we have observed that compressive forces up-regulated *OC/Bglap* expression after only 4 hours of 10% compression but was inhibited by 20% compressive strain. This indicates that elevated magnitudes of compressive forces may inhibit bone formation. Furthermore, in agreement with our results showing magnitude-dependent regulation of *OC/Bglap* expression, *in vivo* studies on distraction osteogenesis have observed up-regulation of *OC/Bglap* during lengthening after osteotomies (Lammens et al., 1998) and down-regulation of *OC/Bglap* at high strains (Meyer et al., 1999).

OPN/SPP1 plays a role in bone regeneration and bone remodeling. In addition, it is proposed that OPN/SPP1 may be involved in inhibition of the pathologic calcification of the bone (Bilezikian et al., 2002; Saad et al., 2007). ON/SPARC is a very important factor during bone mineralization (Hall, 2005). The observation that OPN/SPP1 and ON/SPARC were significantly up-regulated by compressive forces suggests that compressive forces regulate bone matrix synthesis and mineralization. Interestingly, up-regulation of OPN/SPP1 expression in osteoblastic cell monolayer cultures has also been shown by biaxial strain and compressive forces (Mitsui et al., 2005; Toma et al., 1997).

Overall, our findings demonstrate that compressive forces are osteogenic and act on bone cells in a magnitude-dependent manner and provide a possible molecular model for the increased bone strength observed in response to physical activity. The insight into the molecular mechanisms involved in the cellular responses to appropriate levels of biomechanical forces suggests that these forces are important to improve fracture healing. Additionally, these findings may provide a partial explanation for the loss of bone strength in response to excessive mechanical forces. While further work is needed to fully dissect the pathways involved in the regulation of osteogenesis by mechanical forces, our data provides critical insights into the possible molecular mechanisms of action necessary.

Acknowledgements

The authors are thankful to Dr. Y. Ha (University of Nebraska) and Dr. F.M. Beck for their valuable advice on the statistical analysis. This study was supported by grants from the National Institutes of Health: NCCAM AT000646, NIDCR DE015399, and NIAMS AR048781.

References

- Bikle DD, Halloran BP. The response of bone to unloading. *Journal of Bone and Mineral Metabolism* 1999;17:233–244. [PubMed: 10575587]
- Bilezikian, JP.; Raisz, LG.; Rodan, GA., editors. *Principles of bone biology*. 2. Academic Press; California: 2002.
- Cao T, Ho KH, Teoh SH. Scaffold design and in vitro study of osteochondral coculture in a three-dimensional porous polycaprolactone scaffold fabricated by fused deposition modeling. *Tissue Engineering* 2003;9:103–109.
- Cartmell SH, Porter BD, García AJ, Gulberg RE. Effects of medium perfusion rate on cell-seeded three-dimensional bone constructs in vitro. *Tissue Engineering* 2003;9:1197–1203. [PubMed: 14670107]
- Chao EY, Inoue N, Elias JJ, Aro H. Enhancement of fracture healing by mechanical and surgical intervention. *Clinical Orthopaedics and Related Research* 1998;355:163–178. [PubMed: 9917601]
- Cowin SC. Bone poroelasticity. *Journal of Biomechanics* 1999;32:217–238. [PubMed: 10093022]
- Damsky CH. Extracellular matrix-integrin interactions in osteoblast function and tissue remodeling. *Bone* 1999;25:181–190.
- Deschner J, Rath-Deschner B, Agarwal S. Regulation of matrix metalloproteinase expression by dynamic tensile strain in rat fibrochondrocytes. *Osteoarthritis and Cartilage* 2006;14:264–272. [PubMed: 16290189]
- ten Dijke P. Bone morphogenetic protein signal transduction in bone. *Current Medical Research and Opinion* 2006;22:7–11.
- Ducy P, Zhang R, Geoffroy V, Ridall AL, Karsenty G. *Osf2/Cbfa1*: A transcriptional activator of osteoblast differentiation. *Cell* 1997;89:747–754. [PubMed: 9182762]
- Ducy P. The osteoblast: A sophisticated fibroblast under central surveillance. *Science* 2000;289:1501–1504. [PubMed: 10968779]
- Duty AO, Oest ME, Gulberg RE. Cyclic mechanical compression increases mineralization of cell-seeded polymer scaffolds in vivo. *Journal of Biomechanical Engineering* 2007;129:531–539. [PubMed: 17655474]
- Egger EL, Gottsauner-Wolf F, Palmer J, Aro HT, Chao EY. Effects of axial dynamization on bone healing. *The Journal of Trauma* 1993;43:185–192. [PubMed: 8459454]
- Ehrlich PJ, Lanyon LE. Mechanical strain and bone cell function: A review. *Osteoporosis International* 2002;13:688–700. [PubMed: 12195532]
- Einhorn TA. The cell and molecular biology of fracture healing. *Clinical orthopaedics and Related Research* 1998;355:7–21.
- Fernández-Tresguerres-Hernández-Gil I, Alobera-Gracia MA, del-Canto-Pingarrón M, Blanco-Jerez L. Physiological bases of bone regeneration I. histology and physiology of bone tissue. *Medicina oral, patología oral y cirugía bucal* 2006;11:47–51.

- Gabbay JS, Zuk PA, Tahernia A, et al. In vitro microdistraction of preosteoblasts: Distraction promotes proliferation oscillation promotes differentiation. *Tissue Engineering* 2006;12:3055–3065. [PubMed: 17518621]
- Gardner MJ, van der Meulen MC, Demetrakopoulos D, Wright TM, Myers ER, Bostrom MP. In vivo cyclic axial compression affects bone healing in the mouse tibia. *Journal of Orthopaedic Research* 2006;24:1679–1686. [PubMed: 16788988]
- Goodship AE, Cunningham JL, Kenwright J. Strain rate and timing of stimulation in mechanical modulation of fracture healing. *Clinical Orthopaedics and Related Research* 1998;355:105–115.
- Govender S, et al. Recombinant human bone morphogenetic protein-2 for treatment of open tibial fractures: A prospective, controlled, randomized study of four hundred and fifty patients. *The Journal of Bone and Joint Surgery. American Volume* 2002;84:2123–2134.
- Hall, BK., editor. *Bones and cartilage*. Elsevier Academic Press; San Diego: 2005.
- Harada H, Tagashira S, Fujiwara M, Ogawa S, Katsumata T, Yamaguchi A, Komori T, Nakatsuka M. Cbfa1 Isoforms Exert Functional Differences in Osteoblast Differentiation. *The Journal of Biological Chemistry* 1999;274:6972–6978. [PubMed: 10066751]
- Ishaug SL, Crane GM, Miller MJ, Yasko AW, Yaszemski MJ, Mikos AG. Bone formation by three-dimensional stromal osteoblast culture in biodegradable polymer scaffolds. *Journal of Biomedical Material Research* 1997;36:17–28.
- Jeon EJ, Lee KY, Choi NS, et al. Bone morphogenetic protein-2 stimulates Runx2 acetylation. *The Journal of Biological Chemistry* 2006;281:16502–16511. [PubMed: 16613856]
- Johnson J, Gosh A, Lannutti JJ. Microstructure-Property Relationships in a Tissue Engineering Scaffold. *Journal of Applied Polymer Science* 2007;204:2919.
- Kaspar D, Seidl W, Neidlinger-Wilke C, Ignatius A, Claes L. Dynamic Cell stretching increases human osteoblast proliferation and CICP synthesis but decreases osteocalcin synthesis and alkaline phosphatase activity. *Journal of Biomechanics* 2000;33:45–51. [PubMed: 10609517]
- Kenwright J, Goodship AE. Controlled mechanical stimulation in the treatment of tibial fractures. *Clinical Orthopaedics and Related Research* 1989;241:36–47. [PubMed: 2924478]
- Kinoshita S, Finnegan M, Bucholz RW, Mizuno K. Three-dimensional collagen gel culture promotes osteoblastic phenotype in bone marrow derived cells. *The Kobe Journal of Medical Sciences* 1999;45:201–11. [PubMed: 10853186]
- Klein-Nulend J, Veldhuijzen JP, de Jong M, Burger EH. Increased bone formation and decreased bone resorption in fetal mouse calvaria as a result of intermittent compressive force in vitro. *Bone and Mineral* 1987;2:441–448. [PubMed: 3505768]
- Klein-Nulend J, Roelofsens J, Semeins CM, Bronckers AL, Burger EH. Mechanical stimulation of osteopontin mRNA expression and synthesis in bone cell cultures. *J Journal of cellular physiology* 1997;179:174–181.
- Klein-Nulend J, Bacabac RG, Mullender MG. *Mechanobiology of bone tissue*. Pathologie-Biologie (Paris) 2005;53:567–580.
- Koike M, Shimokawa H, Kanno Z, Ohya K, Soma K. Effects of mechanical strain on proliferation and differentiation of bone marrow stromal cell line ST2. *Journal of Bone and Mineral Metabolism* 2005;23:219–225. [PubMed: 15838624]
- Lammens J, Liu Z, Aerssens J, Dequeker J, Fabry G. Distraction bone healing versus osteotomy healing: A comparative biochemical analysis. *Journal of Bone and Mineral Research* 1998;13:279–86. [PubMed: 9495522]
- Lee KS, Kim HJ, Li QL, et al. Runx2 is a common target of transforming growth factor beta 1 and bone morphogenetic protein 2, and cooperation between Runx2 and Smad5 induces osteoblast-specific gene expression in the pluripotent mesenchymal precursor cell line C2C12. *Molecular and Cellular Biology* 2000;20:8783–8792. [PubMed: 11073979]
- Lian JB, Javed A, Zaidi SK, et al. Regulatory controls for osteoblast growth and differentiation: Role of Runx/Cbfa/AML factors. *Critical reviews in eukaryotic gene expression* 2004;14:1–41. [PubMed: 15104525]
- Livak KJ, Schmittgen TD. Analysis of relative gene expression data using real-time quantitative PCR and the 2(-delta delta C(T)) method. *Methods* 2001;25:402–408. [PubMed: 11846609]

- Luna, LG. Manual of histologic staining methods of the Armed Forces Institute of Pathology. 3. McGraw-Hill; New York: 1968.
- MacKelvie KJ, Khan KM, Petit MA, Janssen PA, McKay HA. A school-based exercise intervention elicits substantial bone health benefits: A 2-year randomized controlled trial in girls. *Pediatrics* 2003;112:447. [PubMed: 12897308]
- Masi L, Franchi A, Santucci M, et al. Adhesion, growth and matrix production by osteoblasts on collagen substrata. *Calcified Tissue International* 1992;51:202–212. [PubMed: 1330236]
- Meyer U, Meyer T, Vosshans J, Joos U. Decreased expression of osteocalcin and osteonectin in relation to high strains and decreased mineralization in mandibular distraction osteogenesis. *Journal of Cranio-maxillo-facial Surgery* 1999;27:222–227. [PubMed: 10626255]
- Mikuni-Takagaki Y, Suzuki Y, Kawase T, Saito S. Distinct responses of different populations of bone cells to mechanical stress. *Endocrinology* 1996;137:2028–2035. [PubMed: 8612544]
- Mitsui N, Suzuki N, Maeno M, et al. Optimal compressive force induces bone formation via increasing bone sialoprotein and prostaglandin E(2) production appropriately. *Life Sciences* 2005;77:3168–3182. [PubMed: 16055156]
- Nam J, Huang Y, Agarwal S, Lannutti JJ. Improved cellular infiltration in electrospun fiber via engineered porosity. *Tissue Engineering* 2007a;13:2249–2257. [PubMed: 17536926]
- Nam J, Huang Y, Agarwal S, Lannutti JJ. Materials Selection and Residual Solvent Retention in Biodegradable Electrospun Fibers. *Journal of Applied Polymer Science*. 2007bin print
- Phillips AM. Overview of the fracture healing cascade. *Injury* 2005;36:5–7.
- Roelofsen J, Klein-Nulend J, Burger EH. Mechanical stimulation by intermittent hydrostatic compression promotes bone-specific gene expression in vitro. *Journal of Biomechanics* 1995;28:1493–1503. [PubMed: 8666589]
- Rubin C, Turner AS, Bain S, Mallinckrodt C, McLeod K. Low mechanical signals strengthen long bones. *Nature* 2001;412:603–604. [PubMed: 11493908]
- Rubin J, Rubin C, Jacobs CR. Molecular pathways mediating mechanical signaling in bone. *Gene* 2006;367:1–16. [PubMed: 16361069]
- Ryoo HM, Lee MH, Kim YJ. Critical molecular switches involved in BMP-2-induced osteogenic differentiation of mesenchymal cells. *Gene* 2006;366:51–57. [PubMed: 16314053]
- Saad FA, Salih E, Glimcher MJ. Identification of osteopontin phosphorylation sites involved in bone remodeling and inhibition of pathological calcification. *Journal of cellular biochemistry*. 2007 July 5, 2007;Epub ahead of print
- Tanaka SM, Sun HB, Roeder RK, Burr DB, Turner CH, Yokota H. Osteoblast responses one hour after load-induces fluid flow in a three-dimensional porous matrix. *Calcified Tissue International* 2005;76:261–271. [PubMed: 15812578]
- Toma CD, Ashkar S, Gray ML, Schaffer JL, Gerstenfeld LC. Signal transduction of mechanical stimuli is dependent on microfilament integrity: Identification of osteopontin as a mechanically induced gene in osteoblasts. *Journal of Bone and Mineral Research* 1997;12:1626–1636. [PubMed: 9333123]
- Visconti LA, Yen EHK, Johnson RB. Effect of strain on bone nodule formation by rat osteogenic cells in vitro. *Archives of Oral Biology* 2004;49:485–492. [PubMed: 15099806]
- Wan M, Cao X. BMP signaling in skeletal development. *Biochemical and Biophysical Research Communications* 2005;328:651–657. [PubMed: 15694398]
- Ziros PG, Gil AP, Georgakopoulos T, et al. The bone-specific transcriptional regulator *cbfa1* is a target of mechanical signals in osteoblastic cells. *The Journal of Biological Chemistry* 2002;277:23934–23941. [PubMed: 11960980]

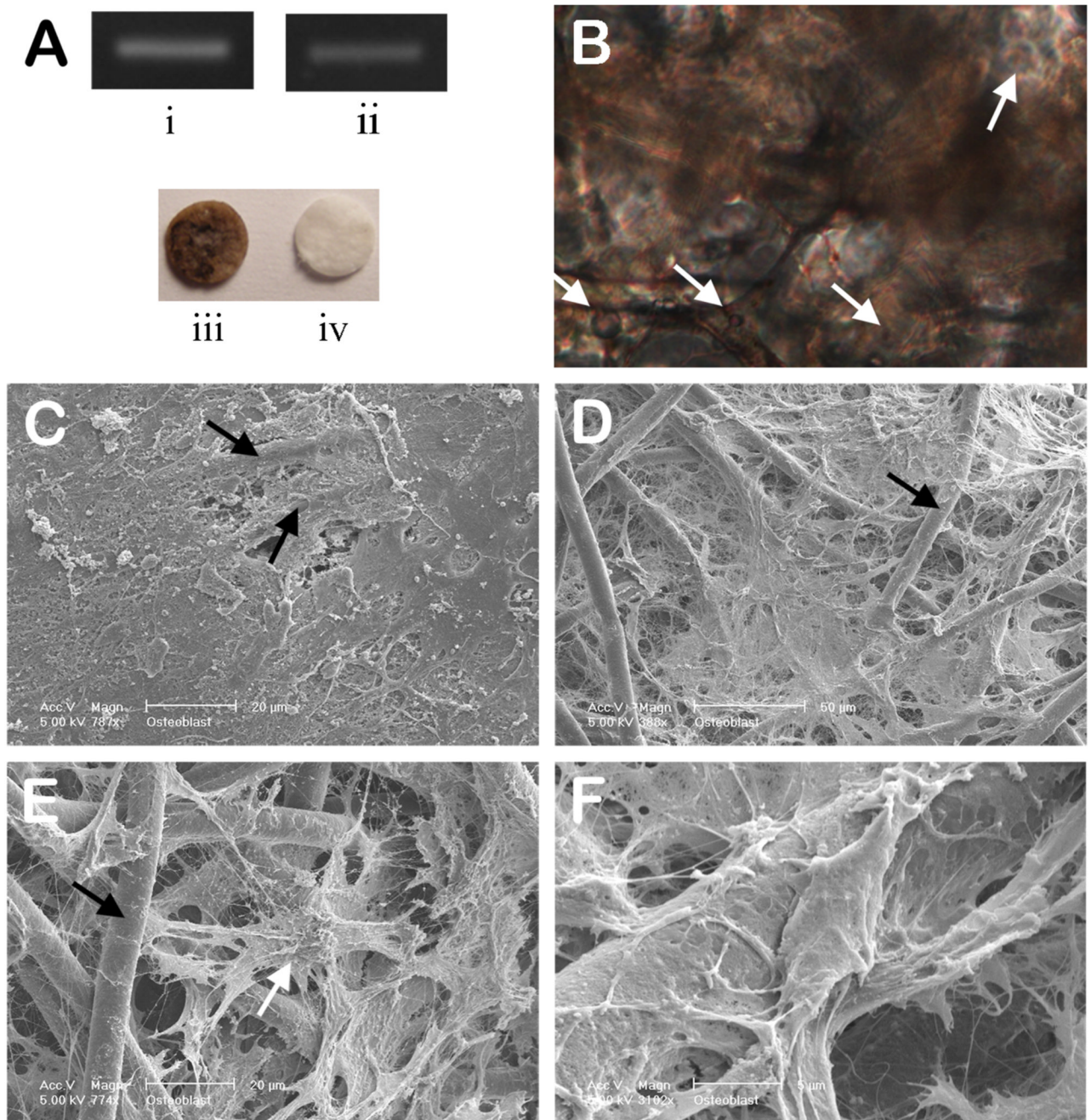


Figure 1.

(A) Constitutive expression of phenotypic mRNA for (i) *Akp2* and (ii) *OC/Bglap* in long-term cultured osteoblasts in 3-D PCL scaffolds, as analyzed by endpoint RT-PCR. Optical image of von Kossa stained (iii) 3-D cell-scaffold construct cultured for 4 weeks and (iv) an acellular control scaffold. Representative data from three separate experiments are shown. (B) A cross-section of a cell-scaffold construct stained with von Kossa and nuclear fast red after 4 weeks culture showing extensive mineralization (200X). (C-F) SEM images of cell/scaffold constructs cultured for 4 weeks; (C) the surface of the construct showing extensive matrix deposition, (D-F) the internal microstructure of the scaffold/cell constructs showing (D) ECM deposition surrounding osteoblasts and PCL fibers, (E) osteoblast integrated in an ECM and

PCL-fiber network, and (F) high magnification image of fibrous ECM connected to a PCL fiber (white arrow: osteblast, black arrow: PCL fiber).

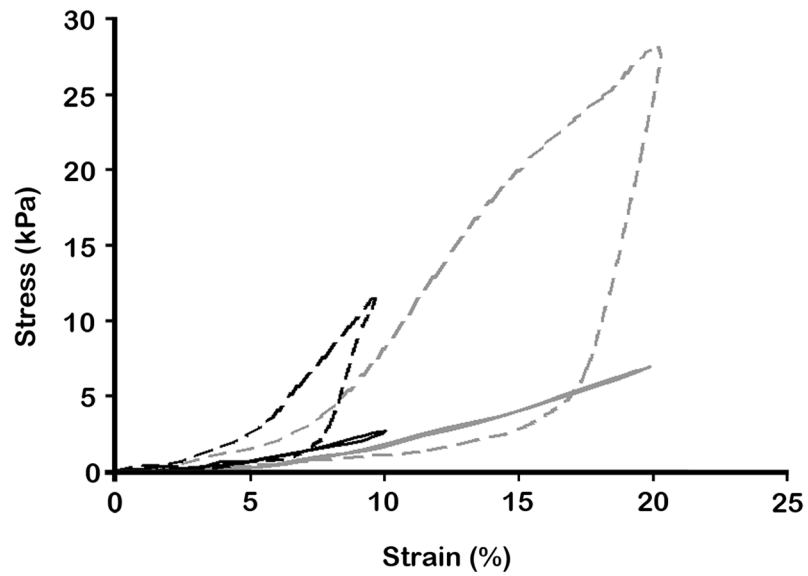


Figure 2. Stress-Strain graph of acellular scaffolds and 4 week-cultured osteoblast-scaffold constructs. 10 or 20% compressive strain at 0.5 Hz with a saw-tooth profile was applied to the scaffolds or cell-scaffold constructs, and responding stress variations were monitored. Black and gray lines represent 10 and 20% compressed samples, respectively. Dashed lines represent cell-scaffold constructs after 4 weeks culture. The graph shows increased Young's moduli in cell cultured scaffolds compared to acellular scaffolds.

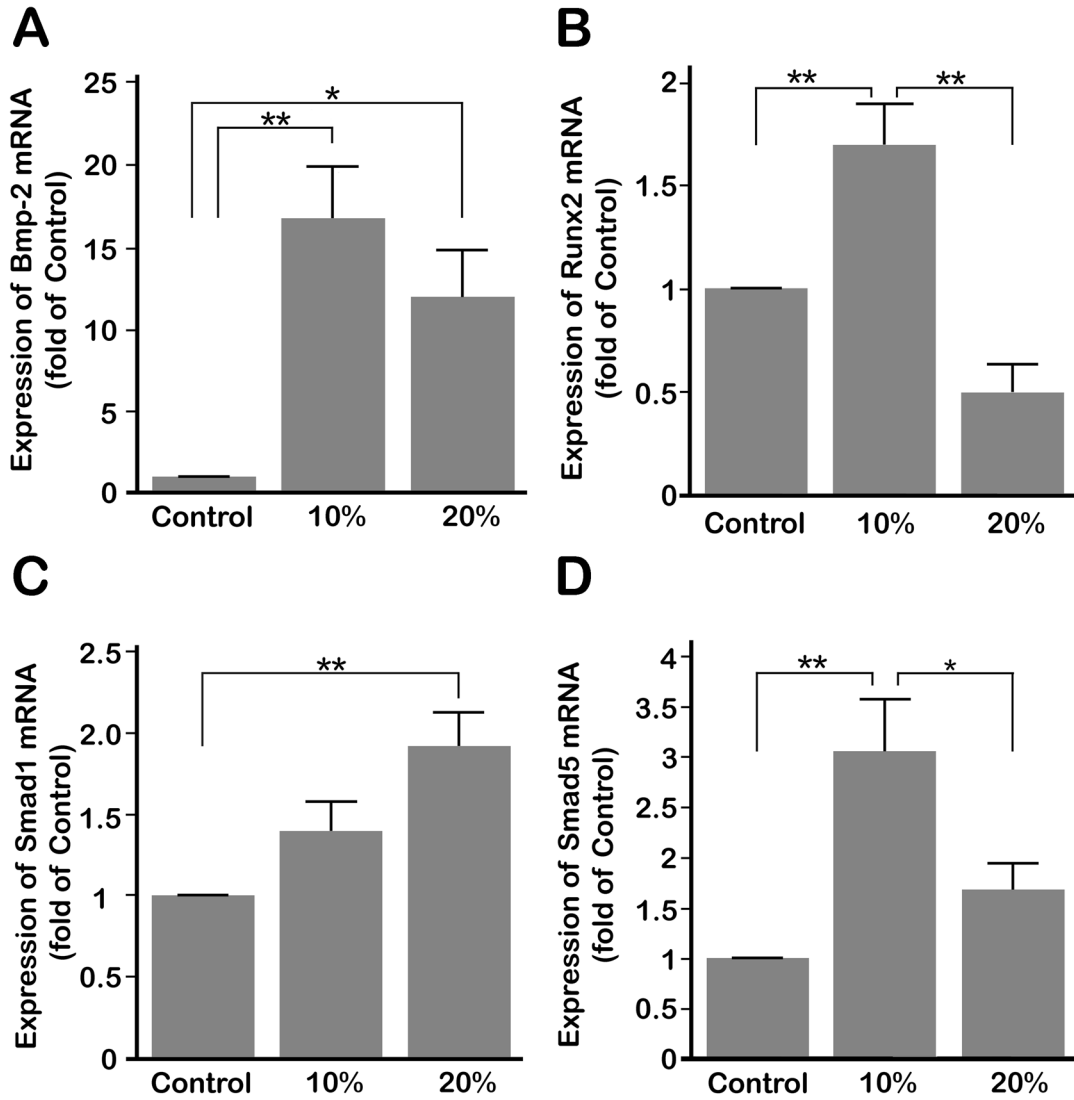


Figure 3.

(A) *Bmp-2* mRNA shows significantly higher levels of expression after 4 hours of 10 or 20% compressive strains at 0.5 Hz over control cells. No significant difference was observed between 10 and 20% compressive strain. (B) *Runx2* mRNA was significantly up-regulated under 4 hours of compressive strain at 0.5 Hz compared to both control and 20% compression treated cells. (C) Both compressive magnitudes showed increased *Smad1* mRNA expression, the gene expression after 20% compression was significant over control. (D) *Smad5* mRNA was significantly up-regulated under 4 hours of 10% compression at 0.5 Hz compared to control and 20% compression treated cells. Bars represent mean \pm SEM (n=6). Significant differences among the groups are noted by * ($p < 0.05$) and ** ($p < 0.01$).

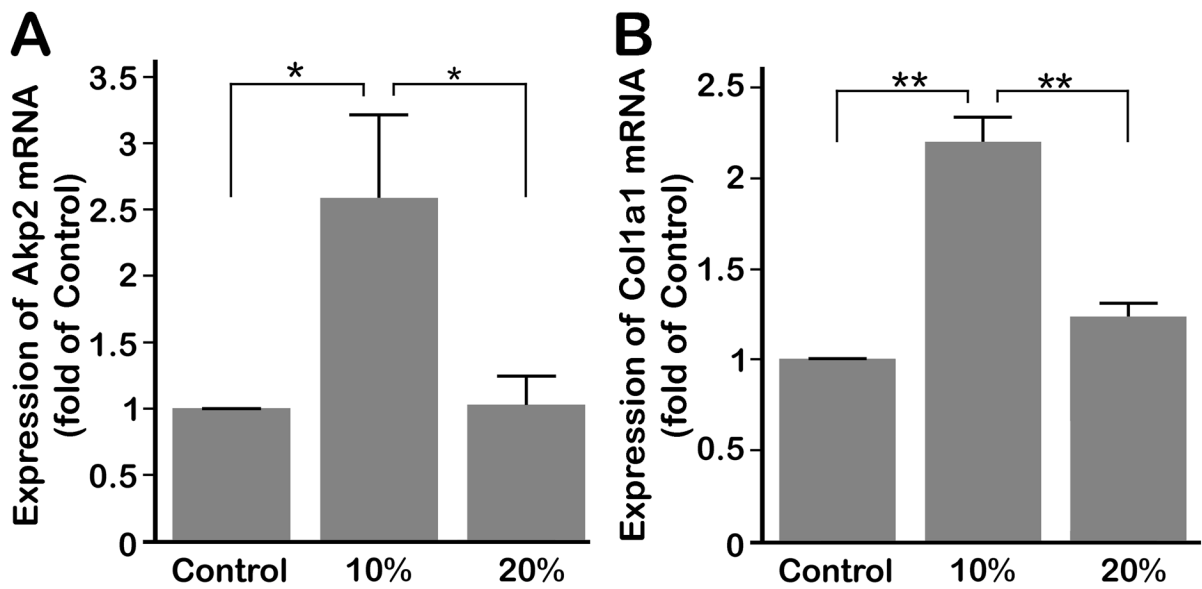


Figure 4.

(A) Significant up-regulation of *Akp2* mRNA under 4 hours of 10% compressive strain at 0.5 Hz compared to control and 20% strain treated cells. (B) Significant up-regulation of *Col1a1* by 10% compressive strain over control and 20%. Bars represent mean \pm SEM (n=6). Significant differences among the groups are noted by * ($p < 0.05$) and ** ($p < 0.01$).

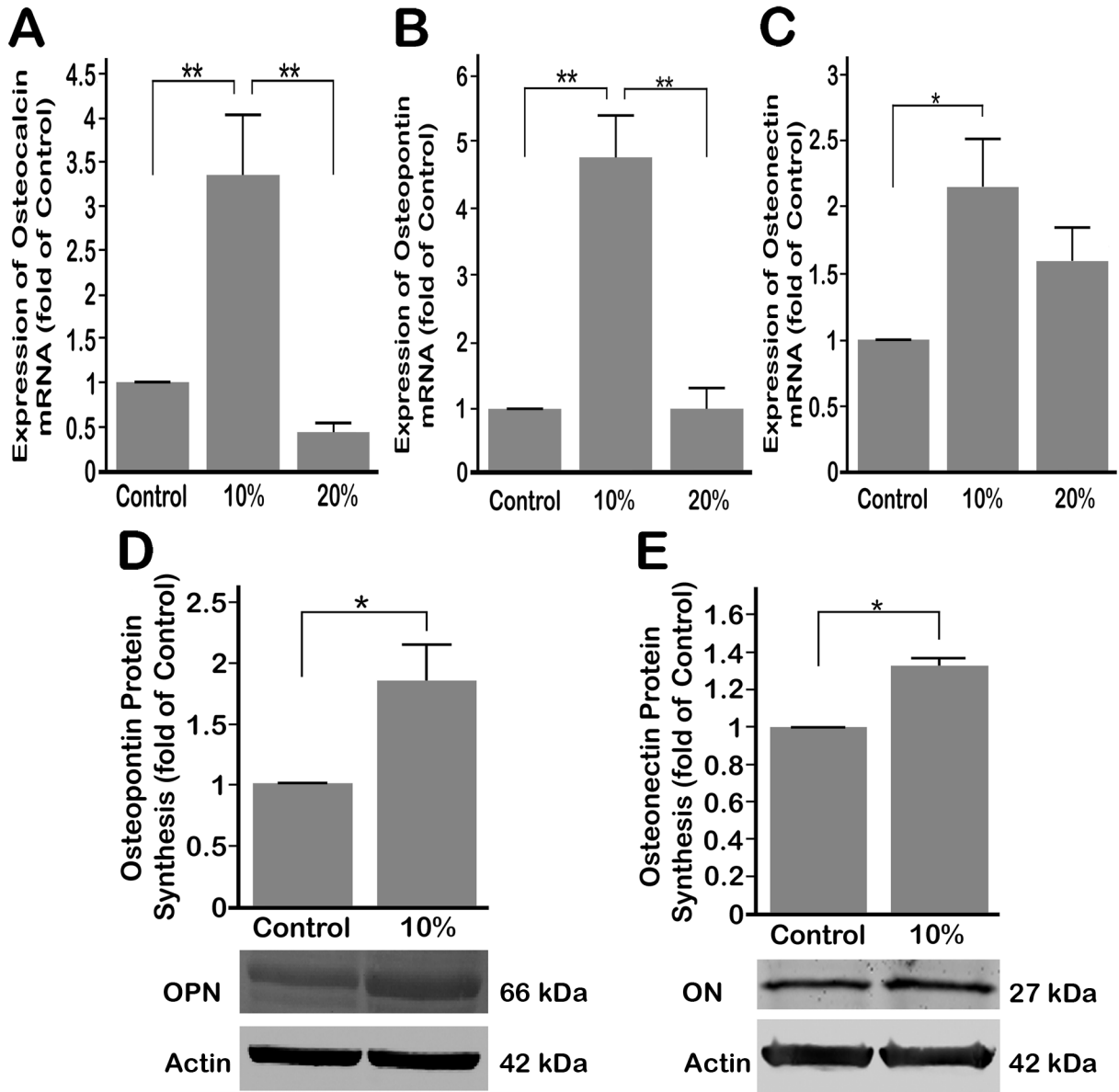


Figure 5. (A) *OC/Bglap* mRNA expression was significantly up-regulated by 4 hours of 10% compressive strain at 0.5 Hz, whereas 20% compressive strain down-regulated *OC/Bglap* mRNA compared to control. (B) *OPN/Spp1* mRNA expression was significantly up-regulated by 4 hours of 10% compressive strain at 0.5 Hz over control and 20% strain treated cells while no significant up-regulation was shown in 20% compression over control cells. (C) *ON/Sparc* mRNA expression showed significant up-regulation under 4 hours of 10% compressive strain at 0.5 Hz over control, whereas 20% compressive strain did not significantly change *ON/Sparc* mRNA expression over control cells. (D) Protein synthesis of OPN/SPP1 shows significant up-regulation after 4 hours of 10% compressive strain followed by 8 hours of rest over control cells. (E) Protein synthesis of *ON/Sparc* after 4 hours of 10% compressive strain at 0.5 Hz increased significantly over control cells. Bars represent mean \pm SEM; (A), (B) and (C) n=6, (D) and (E) n=3. Significant differences among the groups are noted by * ($p < 0.05$) and ** ($p < 0.01$).

Table I

Primer sequences for RT-PCR

	Sense (5'-3')	Antisense (5'-3')	Length (bp)	GenBank Accession
AKP2	CAC AGC CAT CCT GTA TGG CAA	ATG TGG CGG TCT TTG CCA A	162	NM_013059
COL1A1	CCG CCT GAA TAA GGC TGT CAT	ATC TCG CCT GCC ATT CCT T	175	NM_053356
OC/BGLAP	ACT CCG GCG CTA CCT CAA CAA T	ATT GTG ACG AGC TAG CGG ACC A	114	NM_013414
BMP-2	AAC ACC GTG CTC AGC TTC CAT	TTC GGG AAC AAA TGC AGG AA	159	NM_017178
ON/SPARC	TTC TTT GCG ACC AAG TGC ACC	GCG TGA CTG GCT CAA AAA CGT	149	NM_012656
OPN/SPP1	GCC GAG GTG ATA GCT TGG CTT A	TCC GAT GAG GCT ATC AAG GTC A	141	NM_012881
SMAD1	CAT GGC TTT CAT CCC ACC ACG GTC	GCA TGG CCC TCT CCA GTG GCT G	252	NM_013130
SMAD5	TCA ACC ATC GAG AAC ACC AGG	GCA ACT TTC ACC ATG GCT TCC	139	AB010955
RUNX2	TCA CAA ATC CTC CCC AAG TGG	GTG ATT TAG GGC GCA TTC CTC A	151	XM_001066956
RPS18	GCG GCG GAA AAT AGC CTT CG	CAG CAC ACC AAG ACC ACT GGC C	356	NM_213557